

Nuclear structure aspects in the decay of odd medium mass composite systems formed in the reactions with $E/A = 8$ MeV

Manpreet Kaur and BirBikram Singh

Abstract—The decay of odd medium mass composite systems $^{179}\text{Re}^*$ and $^{189}\text{Au}^*$ formed in $^{20}\text{Ne}+^{159}\text{Tb}$, $^{20}\text{Ne}+^{169}\text{Tm}$ reactions, respectively, have been analyzed within the Quantum mechanical fragmentation theory based Dynamical Cluster Decay Model. In the present work, the nuclear structure aspects of decaying composite systems which perforate the spectroscopic factor P_0 (preformation probability) via the fragmentation potential of different fragments within the collective clusterization process have been explored. The results show that evaporation residues (ER) and the fission are the probable decay modes. Also, for both the odd mass composite systems with small change in mass, formed in the reactions with same projectile ^{20}Ne with bombarding energy $E/A = 8$ MeV and same entrance channel mass asymmetry ($\eta \sim 0.77$), the decay probability into LP, fission fragments is affected, comparatively. In both the composite systems, the ER cross-section is more in case of $^{179}\text{Re}^*$ comparatively. Also, the presence of two fission windows, the symmetric fission (SF) and asymmetric fission or heavy mass fragments (HMF), suggest the possibility of sub-structure of fission fragments. Also, the disagreement between DCM calculated fission cross-section and data, in both the reactions, suggests that there may be the effects of non-compound nucleus process (i.e. quasi fission) whose contribution has been evaluated empirically. It is to be noted that with same value of neck length parameter (ΔR), fitted simultaneously for ER and fission fragments for one of reactions, we are able to fit the experimental ER and fission cross-section for second reaction.

Index Terms—evaporation residues, fission, quasi fission, dynamical cluster decay model

I. INTRODUCTION

The study of decay of composite system formed in heavy ion reactions at low energy facilitates to understand the intricate process of fusion of two

heavy nuclei. The decay process involve the emission of light particles (LP) ($A \leq 4$, $Z \leq 2$) leading to evaporation residues (ER) along with emission of intermediate mass fragments (IMF) and fusion-fission (ff) which comprises of symmetric fragments (SF) and/or heavy mass fragments (HMF) depending upon the mass, excitation energy and angular momentum of composite system formed. Also, there may be effect of non-compound nucleus process such as quasi fission (QF), deep inelastic collision (DIC), pre-equilibrium emission etc. playing the role in the reaction mechanism.

The studies show that the medium mass composite systems (CS) decay by the emission of ER and fission. The decay of medium mass CS $^{164}\text{Yb}^*$, $^{200,202}\text{Pb}^*$ and $^{176,182,188,196}\text{Pt}^*$ have been studied successfully within the formalism of Dynamical Cluster decay Model (DCM) [1,2]. DCM is based on well established quantum mechanical fragmentation theory, in which the decay of compound nucleus into LP, IMF, HMF and ff is treated on the equal footing unlike in case of statistical models.

The ER and fission cross-sections for $^{179}\text{Re}^*$ and $^{189}\text{Au}^*$, formed in $^{20}\text{Ne}+^{159}\text{Tb}$ and $^{20}\text{Ne}+^{169}\text{Tm}$ reactions with projectile energy $E/A = 8, 10, 13, 16$ MeV, have been measured [3]. It is interesting to explore the dynamics of these odd mass CS formed in the reactions with same projectile (^{20}Ne) energy per nucleon i.e. $E/A = 8$ MeV. Also, the entrance channel mass asymmetry in both the reactions is similar ($\eta \sim 0.77$). The decay of $^{179}\text{Re}^*$ formed in $^{20}\text{Ne}+^{159}\text{Tb}$ reaction with $E/A=8$ MeV has been studied within DCM. Also, the decay of $^{189}\text{Au}^*$ formed in $^{20}\text{Ne}+^{169}\text{Tm}$ reaction has been explored comparatively [4,5]. In the present work, the nuclear structure aspects of these decaying CS are explored via preformation probability of different fragments, which in turn depends on the fragmentation potential of different fragments calculated within the collective clusterization process of DCM. Also, the LP and fission cross-sections have been estimated and compared with experimental data by fitting the neck

Sri Guru Granth Sahib World University, Fatehgarh Sahib - 140406, India (e-mail(s): manpreet13phd@srgswu.edu.in, birbikramsingh@srgswu.edu.in)

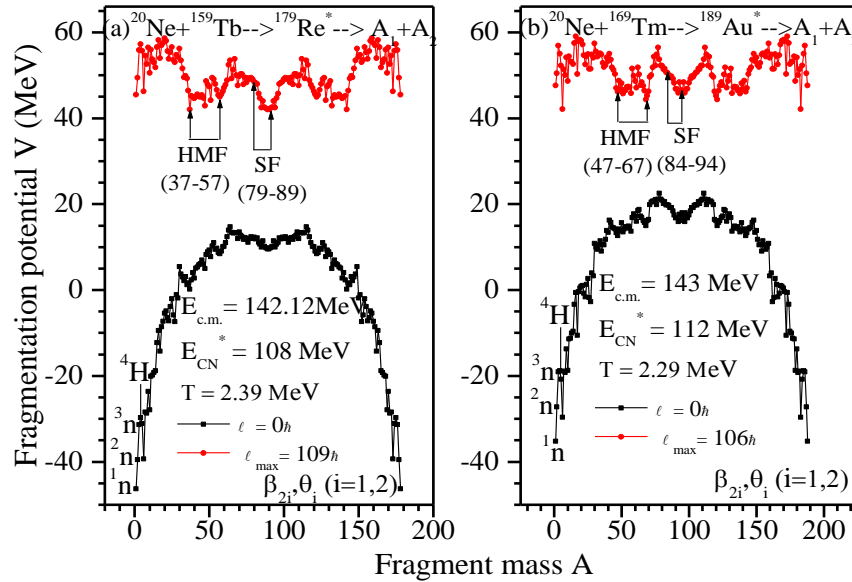


Fig. 1. Variation of fragmentation V (MeV) with the fragment mass for the decay of (a) $^{179}\text{Re}^*$ (b) $^{189}\text{Au}^*$ formed in $^{20}\text{Ne}+^{159}\text{Tb}$, $^{20}\text{Ne}+^{169}\text{Tm}$ reactions respectively, with projectile energy $E/A = 8$ MeV, at simultaneous fitted values of $\Delta R_{LP} = 1.99$ fm, $\Delta R_{SF} =$ and $\Delta R_{HMF} = 1.32$ fm. The fragments contributing to fission i.e. symmetric fragments (SF) and asymmetric fragments/ heavy mass fragments (HMF) are also shown in the figure.

length parameter (ΔR).

II. METHODOLOGY-DYNAMICAL CLUSTER DECAY MODEL

In the present study, the decay of hot and rotating compound system formed in heavy ion reaction is studied within the framework of DCM of Gupta and collaborators [2]. DCM, based on quantum mechanical fragmentation theory (QMFT), is worked out in the terms of collective coordinates of (i) mass asymmetry $\eta = (A_1 - A_2)/(A_1 + A_2)$ (ii) relative separation R (iii) quadrupole deformations β_{2i} ($i=1,2$) and orientations θ_i of two fragments. In terms of these coordinates, the DCM defines the decay cross-section, in terms of ℓ partial waves, as

$$\sigma = \frac{\pi}{k^2} \sum_{l=0}^{l_{\max}} (2l+1) P_0 P; k = \sqrt{\frac{2\mu E_{c.m.}}{\hbar^2}} \quad \dots(1)$$

where l_{\max} is the maximum angular momentum value for which $\sigma_{LP} \rightarrow 0$. The preformation probability (P_0) in eq. (1) given as

$$P_0 = |\psi_R(\eta(A_i))|^2 \sqrt{B_{\eta\eta}} \frac{2}{A_{CN}} \quad \dots(2)$$

refers to η motion and is obtained by the solution of

Schrödinger equation in η , at a fixed $R=R_a$

$$\left\{ -\frac{\hbar^2}{2\sqrt{B_{\eta\eta}}} \frac{\partial}{\partial \eta} \frac{1}{\sqrt{B_{\eta\eta}}} \frac{\partial}{\partial \eta} + V_R(\eta, T) \right\} \psi^v(\eta) = E^v \psi^v(\eta) \quad \dots(3)$$

with $v = 0,1,2,3\dots$ referring to ground-state ($v = 0$) and excited states solutions. The mass parameter $B_{\eta\eta}$ are the smooth classical hydrodynamical masses [6]. The tunneling probability P in eq. (1), for each η , is calculated as the WKB integral

$$P = \exp\left[-\frac{2}{\hbar} \int_{R_a}^{R_b} \{2\mu[V(R) - Q_{\text{eff}}]\}^{1/2} dR\right] \quad \dots(4)$$

with R_a and R_b as the first and second turning points. Q_{eff} is the Q -value of the decay process and the first turning point R_a defined as:

$$R_a(T) = R_1(\alpha_1, T) + R_2(\alpha_2, T) + \Delta R(\eta, T)$$

where $R_i(\alpha_i) = R_{0i}(T) [1 + \sum \beta_{\lambda i} Y_{\lambda}^{(0)}(\alpha_i)]$ and $R_{0i}(T) = [1.28A^{1/3}_i - 0.76 + 0.8A^{1/3}_i][1 + 0.0007T^2]$.

The fragmentation potential $V(R, \eta, \beta_{\lambda i}, \theta_i, T)$ is the sum of liquid drop energy V_{LDM} , shell corrections δU , Coulomb potential V_c , nuclear proximity V_p and angular momentum dependent potentials V_ℓ , given as:

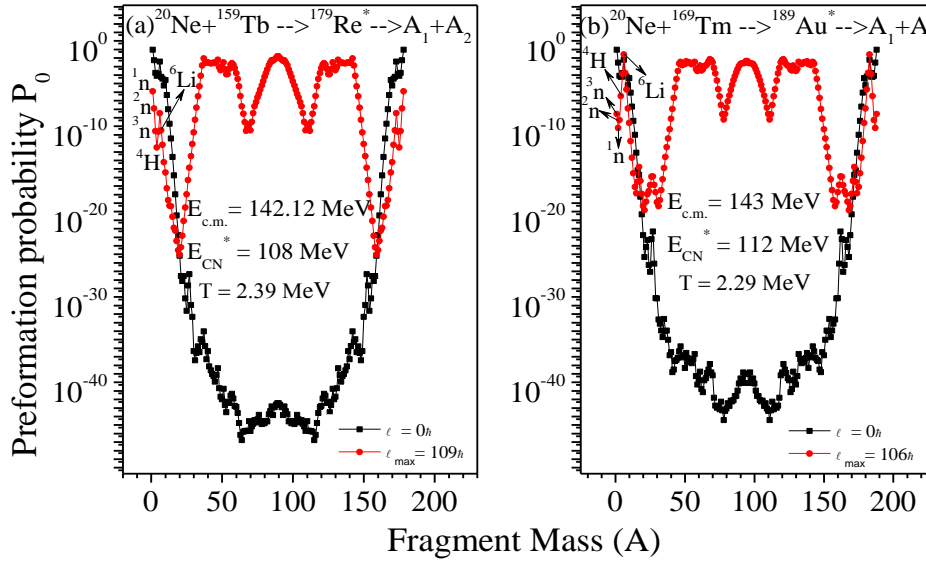


Fig.2: Variation of preformation probability P_0 with fragment mass for the decay of (a) $^{179}\text{Re}^*$ (b) $^{189}\text{Au}^*$ formed in $^{20}\text{Ne} + ^{159}\text{Tb}$, $^{20}\text{Ne} + ^{169}\text{Tm}$ reactions respectively with projectile energy $E/A = 8$ MeV, at simultaneous fitted values of $\Delta R_{LP} = 1.99$ fm, $\Delta R_{SF, HMF} = 1.32$ fm.

$$V_R(\eta, T) = \sum_{i=1}^2 [V_{LDM}(A_i, Z_i, T)] + \sum_{i=1}^2 [\delta U_i] \exp(-T^2 / T_0^2) + V_c(R, Z_i, \beta_{\lambda i}, \theta_i, T) + V_p(R, A_i, \beta_{\lambda i}, \theta_i, T) + V_\ell(R, A_i, \beta_{\lambda i}, \theta_i, T) \quad \dots(5)$$

The contributions of σ_{SF} and σ_{HMF} (using eq. (1)) in total $\sigma_{fission}$ are calculated for the best fit of the only parameter, the neck length parameter ΔR . The contribution of non-compound nucleus process (i.e. of QF in $\sigma_{fission}$ (i.e. $\sigma_{QF} = \sigma_{fission}^{Expt} - \sigma_{fission}^{DCM}$) is calculated empirically.

III. CALCULATIONS AND DISCUSSION

The Fig.1 shows the variation of fragmentation potential with fragment mass (A) in the decay of (a) $^{179}\text{Re}^*$ and (b) $^{189}\text{Au}^*$ at two extreme values of $\ell = 0\hbar$ and their ℓ_{max} values respectively, with consideration of quadrupole deformation effects (β_{2i}) and optimum orientations of hot compact configurations as in table 1 of [7]. For both CS, at $\ell = 0\hbar$, the LP are having lower fragmentation potential compared to IMF, HMF and fission fragments i.e. LP are more favored at $\ell = 0\hbar$ and in both the cases, the LP are n-rich i.e. $^{1,2,3}n$ and 4H . For both the CS, at their respective ℓ_{max} values, there is strong minima for SF ($A = 79-89$ and $A=84-94$, plus the complementary fragments

$A_1 = A_{CN} - A$, respectively for $^{179}\text{Re}^*$ and $^{189}\text{Au}^*$) which represent the SF window with mass $A_{CN}/2 \pm 10$. Also, another minima is observed in the vicinity of the SF window, corresponding to HMF ($A = 37-57$ and $A=47-67$, plus the complementary fragments $A_1 = A_{CN} - A$, respectively for $^{179}\text{Re}^*$ and $^{189}\text{Au}^*$), termed as the HMF window. The occurrence of HMF window, in addition to SF window, suggest the possibility of sub-structure in the fission of $^{179}\text{Re}^*$ and $^{189}\text{Au}^*$. These nuclear structure aspects of decaying CS are further probed via the preformation probability (P_0) in the Fig.2, which shows variation of preformation profile of different fragments in the decay of (a) $^{179}\text{Re}^*$ and (b) $^{189}\text{Au}^*$ at extreme ℓ -values.

In comparison, one observes that for the decay of $^{179}\text{Re}^*$, the maxima is more stronger for SF compared to maxima at asymmetric fission fragments (or HMF), while in the decay of $^{189}\text{Au}^*$, the maxima at asymmetric fission fragments competes with maxima at SF. Also, we note that 6Li (IMF) is having less value of P_0 , in case of $^{179}\text{Re}^*$, at both $\ell = 0\hbar$ and ℓ_{max} values while it is having significant P_0 in case of $^{189}\text{Au}^*$. Thus, the emission of LP and fission fragments (SF and HMF) are significant decay modes for the systems under the present study.

TABLE I

$E_{c.m.}$ (MeV)	E_{CN}^* (MeV)	T (MeV)	ΔR			σ^{DCM}			σ^{Expt}		σ^{Emp}_{QF}	
			LP	HMF	SF	LP	HMF	SF	fission= HMF+SF	LP		fission
$^{20}\text{Ne}+^{159}\text{Tb} \rightarrow ^{179}\text{Re}^* \rightarrow A_1+A_2$												
142.12	108	2.398	1.99	1.32	1.32	703.82	104.14	65.80	169.94	711±46	641±25	471.06
$^{20}\text{Ne}+^{169}\text{Tm} \rightarrow ^{189}\text{Au}^* \rightarrow A_1+A_2$												
143	112	2.295	1.99	1.32	1.32	334.64	36.26	8.46	44.72	351±59	1070±41	1025.28

The DCM calculated cross-sections for LP, HMF and SF calculated within DCM, for the decay of $^{179}\text{Re}^*$ and $^{189}\text{Au}^*$ formed in the reactions with $E/A = 8$ MeV and comparison with the experimental data (σ^{Expt}) [3]. The σ^{Emp}_{QF} is the empirically calculated value of quasi fission.

Further, we look for penetrability of different fragments which contributes to the cross-section of LP, HMF and SF (acc. to eq. (1)). The cross-sections calculated, within DCM, by simultaneous fitting of neck length parameter ΔR for LP, HMF, SF are shown in Table I along with comparison with experimental data [3]. The σ_{DCM} are the calculated cross-sections, within DCM, of LP, fission which is having contribution from SF and HMF.

For both the reactions, leading to the CS with small difference in mass, there is large difference in magnitude of LP cross-section comparatively, the σ_{LP}^{DCM} in $^{179}\text{Re}^*$ is having the double magnitude than in case of $^{189}\text{Au}^*$. With same value of ΔR_{LP} , we are able to account for the experimental LP cross-section data for both the reactions. The fission cross-section comprises of contributions from asymmetric fission fragments (or HMF) and SF (as shown in Fig. 1). The HMF contribute more to the calculated $\sigma_{fission}^{DCM}$ than SF in both CS. In $^{179}\text{Re}^*$, the SF are having more P_0 than HMF but have less penetration probability P, hence their contribution to fission cross-section is less compared to HMF while in case of $^{189}\text{Au}^*$, the HMF are having more P_0 than SF and enough penetration probability P, hence their contribution to fission cross-section is more than SF. There is large difference in calculated $\sigma_{fission}^{DCM}$ and $\sigma_{fission}^{Expt}$ and this disagreement between DCM calculated fission cross-sections and data may be due to the presence of effect of non-compound nucleus process of QF, which is estimated empirically. Also, the values of ΔR fitted for the cross-section of one reaction works as the whole for the another reaction (both reactions with $\eta \sim 0.77$). These results show that for the reactions having the same projectile with same E/A and fixed entrance channel mass asymmetry, we find that with same values of ΔR fitted simultaneously for ER and fission fragments for one of reactions, we are able to fit the experimental ER and fission cross-section for second reaction. It may be due to η dependence of ΔR value. To establish this fact the calculations at other values of projectile energy are of further interest.

IV. CONCLUSION

The decay of odd medium mass composite systems $^{179}\text{Re}^*$ and $^{189}\text{Au}^*$ formed in the reactions $^{20}\text{Ne}+^{159}\text{Tb}$ and $^{20}\text{Ne}+^{169}\text{Tm}$ respectively, have been studied within the framework of

DCM. The results show that evaporation residues (ER) and the fission are the probable decay modes. For both the odd mass composite systems with small change in mass, formed in the reactions with same projectile ^{20}Ne having bombarding energy $E/A = 8$ MeV, the decay probability into LP, fission fragments is affected comparatively as depicted in cross-section table. In both the CS relatively, the ER cross-section is more in case of $^{179}\text{Re}^*$, almost double that in case of $^{189}\text{Au}^*$. The fission cross-section consists of contribution from the SF window with mass $A_{CN}/2 \pm 10$ and HMF window of $A = 37-57$ and $A=47-67$ (plus the complementary fragments) respectively for $^{179}\text{Re}^*$ and $^{189}\text{Au}^*$, in the vicinity of the SF window. The presence of these two windows suggests the substructure of fission fragments. These nuclear structure aspects in the decaying composite systems are further probed via preformation probability P_0 of different fragments. The results show that in case of $^{179}\text{Re}^*$, the maxima is more stronger for SF compared to maxima at asymmetric fission fragments (or HMF), while in the decay of $^{189}\text{Au}^*$, the maxima at asymmetric fission fragments competes with maxima at SF. Interestingly, we find that for both the systems formed in the reactions with same entrance channel mass asymmetry ($\eta \sim 0.77$), with same value of neck length parameter (ΔR) fitted simultaneously for ER and fission fragments for one of reactions, we are able to fit the experimental ER and fission cross-section for second reaction. The disagreement between DCM calculated fission cross-sections and data may be due to the presence of effect of non-compound nucleus process (QF), which has been evaluated empirically.

REFERENCES

- [1] S. Kanwar et al., (2009) Decay of $^{202}\text{Pb}^*$ formed in $^{48}\text{Ca}+^{154}\text{Sm}$ reaction using the dynamical cluster decay model, Int. J. Mod. Phys. E **18**, 1453 DOI: <http://dx.doi.org/10.1142/S0218301309013725>; S.K. Arun et al., (2009) Fusion–evaporation cross-sections for the $^{64}\text{Ni}+^{100}\text{Mo}$ reaction using the dynamical cluster-decay model, J. Phys. G: Nuc. Part. Phys. **36**, 085105 doi:[10.1088/0954-3899/36/8/085105](https://doi.org/10.1088/0954-3899/36/8/085105); M.K. Sharma et al., (2011) Fusion excitation functions of $^{64}\text{Ni}+^{112-132}\text{Sn}$ reactions studied on the dynamical cluster-decay model, J. Phys. G: Nuc. Part. Phys. **38**, 055104 doi:[10.1088/0954-3899/38/5/055104](https://doi.org/10.1088/0954-3899/38/5/055104); Rajni et al., (2014) Formation and decay of $^{200}\text{Pb}^*$ using different incoming channels, Phys. Rev. C **90**, 044604 DOI: [10.1103/PhysRevC.90.044604](https://doi.org/10.1103/PhysRevC.90.044604).

- [2] R.K. Gupta et al., (2003) Cluster decay of hot $^{56}\text{Ni}^*$ formed in the $^{32}\text{S}+^{24}\text{Mg}$ reaction, Phys. Rev. C **68**, 014610 DOI: [10.1103/PhysRevC.68.014610](https://doi.org/10.1103/PhysRevC.68.014610); (2005) Dynamical cluster-decay model for hot and rotating light-mass nuclear systems applied to the low energy $^{32}\text{S}+^{24}\text{Mg}\rightarrow^{56}\text{Ni}^*$ reaction, Phys. Rev. C **71**, 014601 DOI:[10.1103/PhysRevC.71.014601](https://doi.org/10.1103/PhysRevC.71.014601); (2006) Entrance channel effects in the dynamical cluster decay model for the decay of hot and rotating compound nucleus $^{48}\text{Cr}^*$ at $E_{\text{CN}} \sim 60$ MeV, Int. J. Mod. Phys. E **15**, 699 DOI: [10.1142/S0218301306004521](https://doi.org/10.1142/S0218301306004521); (2008) Decay of $^{246}\text{Bk}^*$ formed in similar entrance channel reactions of $^{11}\text{B}+^{235}\text{U}$ and $^{14}\text{N}+^{232}\text{Th}$ at low energies using the dynamical cluster decay model, Phys. Rev. C **77**, 054613 DOI: [10.1103 PhysRevC.77.054613](https://doi.org/10.1103/PhysRevC.77.054613).
- [3] J. Cabrera et al., (2003) Fusion-fission and fusion-evaporation processes in $^{20}\text{Ne}+^{159}\text{Tb}$ and $^{20}\text{Ne}+^{169}\text{Tm}$ interactions between $E/A=8$ and 16 MeV, Phys. Rev. C **68**, 034613 DOI: [10.1103/PhysRevC.68.034613](https://doi.org/10.1103/PhysRevC.68.034613).
- [4] M. Kaur, B.B. Singh, (2014) Decay of compound system $^{179}\text{Re}^*$ formed in $^{20}\text{Ne}+^{159}\text{Tb}$ reaction using dynamical cluster decay model, DAE Symp. on Nucl. Phys. **59**, 620, available: <http://www.symnp.org/proceedings>.
- [5] M. Kaur, B.B. Singh, (2016) Comparative decay analysis of $^{179}\text{Re}^*$ and $^{189}\text{Au}^*$ formed in the reactions $^{20}\text{Ne}+^{159}\text{Tb}$, ^{169}Tm with $E_{\text{lab}}=8$ MeV/A, DAE Symp. on Nucl. Phys. **61**, 588, available: <http://www.symnp.org/proceedings>.
- [6] H. Kroger, W. Scheid, (1980) Classical model for mass transfer in heavy ion collisions, Jour. of Phys. G **6**, L85, <http://iopscience.iop.org/article/10.1088/0305-4616/6/4/006>.
- [7] R.K. Gupta et al., (2005) Optimum orientations of deformed nuclei for cold synthesis of super-heavy elements and the role of higher multipole deformations, J. Phys. G: Nucl. Part. Phys. **31**, 631 doi:[10.1088/0954-3899/31/7/009](https://doi.org/10.1088/0954-3899/31/7/009).